

---

3-29-2011

## Dynamics of Hyporheic Flow and Heat Transport Across a Bed-to-Bank Continuum in a Large Regulated River

Katelyn E. Gerecht  
*Smith College*

M. Bayani Cardenas  
*The University of Texas at Austin*

Andrew J. Guswa  
*Smith College, aguswa@smith.edu*

Audrey H. Sawyer  
*The University of Texas at Austin*

John D. Nowinski  
*The University of Texas at Austin*

*See next page for additional authors*

Follow this and additional works at: [https://scholarworks.smith.edu/egr\\_facpubs](https://scholarworks.smith.edu/egr_facpubs)



Part of the [Engineering Commons](#)

---

### Recommended Citation

Gerecht, Katelyn E.; Cardenas, M. Bayani; Guswa, Andrew J.; Sawyer, Audrey H.; Nowinski, John D.; and Swanson, Travis E., "Dynamics of Hyporheic Flow and Heat Transport Across a Bed-to-Bank Continuum in a Large Regulated River" (2011). Engineering: Faculty Publications, Smith College, Northampton, MA. [https://scholarworks.smith.edu/egr\\_facpubs/33](https://scholarworks.smith.edu/egr_facpubs/33)

This Article has been accepted for inclusion in Engineering: Faculty Publications by an authorized administrator of Smith ScholarWorks. For more information, please contact [scholarworks@smith.edu](mailto:scholarworks@smith.edu)

---

**Authors**

Katelyn E. Gerecht, M. Bayani Cardenas, Andrew J. Guswa, Audrey H. Sawyer, John D. Nowinski, and Travis E. Swanson

## Dynamics of hyporheic flow and heat transport across a bed-to-bank continuum in a large regulated river

Katelyn E. Gerecht,<sup>1</sup> M. Bayani Cardenas,<sup>2</sup> Andrew J. Guswa,<sup>1</sup> Audrey H. Sawyer,<sup>2</sup> John D. Nowinski,<sup>2</sup> and Travis E. Swanson<sup>2</sup>

Received 24 July 2010; revised 28 December 2010; accepted 11 January 2011; published 22 March 2011.

[1] The lower Colorado River (LCR) near Austin, Texas is heavily regulated for hydropower generation. Daily water releases from a dam located 23 km upstream of our study site in the LCR caused the stage to fluctuate by more than 1.5 m about a mean depth of 1.3 m. As a result, the river switches from gaining to losing over a dam storage-release cycle, driving exchange between river water and groundwater. We assessed the hydrologic impacts of this by simultaneous temperature and head monitoring across a bed-to-bank transect. River-groundwater exchange flux is largest close to the bank and decreases away from the bank. Correspondingly, both the depth of the hyporheic zone and the exchange time are largest close to the bank. Adjacent to the bank, the streambed head response is hysteretic, with the hysteresis disappearing with distance from the bank, indicating that transient bank storage affects the magnitude and direction of vertical exchange close to the bank. Pronounced changes in streambed temperature are observed down to a meter. When the river stage is high, which coincides with when the river is coldest, downward advection of heat from a previous cycles' warm-water pulse warms the streambed. When the river is at its lowest stage but warmest temperature, upwelling groundwater cools the streambed. Future research should consider and focus on a more thorough understanding of the impacts of dam regulation on the hydrologic, thermal, biogeochemical, and ecologic dynamics of rivers and their hyporheic and riparian zones.

**Citation:** Gerecht, K. E., M. B. Cardenas, A. J. Guswa, A. H. Sawyer, J. D. Nowinski, and T. E. Swanson (2011), Dynamics of hyporheic flow and heat transport across a bed-to-bank continuum in a large regulated river, *Water Resour. Res.*, 47, W03524, doi:10.1029/2010WR009794.

### 1. Introduction

[2] Sixty percent of the world's major rivers are dammed for a variety of purposes including hydropower generation, water storage, and recreation [Hancock, 2002; Nilsson *et al.*, 2005]. River regulation by dams has impacts that extend up to hundreds of kilometers downstream, affecting not only riparian environments but also groundwater systems and the hyporheic zone.

[3] The streambed hosts the hyporheic zone, an ecotone where water, nutrients, heat, and contaminants are exchanged between surface water and groundwater systems [Bencala, 2005; Boulton *et al.*, 1998; Hancock, 2002; Vervier *et al.*, 1992]. The hyporheic zone also acts as a protective habitat for many fish and insect eggs and invertebrates [Brunke and Gonser, 1997; Findlay, 1995; Hancock, 2002]. The importance of this zone warrants a full characterization of the impacts of regulation on downstream environments, especially as the fluxes in this zone affect the water quality of both the river and underlying aquifer [Boano *et al.*,

2008; Brunke and Gonser, 1997; Findlay, 1995; Hancock, 2002; Vervier *et al.*, 1992].

[4] The main objective of this study is to advance our understanding of hyporheic zone dynamics when they are subjected to regular stage fluctuations. During the summer of 2009, temperature and pressure measurements were used to identify the depth of the hyporheic zone and to determine how this varies both spatially and temporally. This work provides new insight into hyporheic exchange in a large, regulated river with detailed spatial and temporal resolution and intensity of field observations. The study is unique in its use of hydraulic and thermal measurements to link exchange responses in the streambed and the adjacent bank. A deeper understanding of hyporheic zone hydrology is critical to expanding our current understanding of hyporheic zone ecology and biogeochemistry [Bencala, 2005; Lewandowski *et al.*, 2009]. However, few previous studies have directly estimated hyporheic zone depths using multiple methods, as well as calculated corresponding exchange times. The results of our work provide insight on the effects of regulated releases on hyporheic processes.

### 2. Background

#### 2.1. Previous Related Hyporheic Zone Research

[5] The majority of investigations into river-aquifer interactions have taken place in small, unregulated riparian

<sup>1</sup>Picker Engineering Program, Smith College, Northampton, Massachusetts, USA.

<sup>2</sup>Geological Sciences, University of Texas at Austin, Austin, Texas, USA.

systems. Investigating surface water-groundwater interactions in large rivers is challenging because of the difficulty in instrumentation and data collection in water bodies with deep, fast flows. Nonetheless, these rivers provide habitats for many species, and are often regulated to provide water resources and power for surrounding communities as well as for flood control. Previous research has identified or analyzed the effects of natural stage fluctuations because of diel snowmelt, evapotranspiration, or floods in small meadow streams [Loheide and Lundquist, 2009], mountain streams [Constantz, 1998; Wondzell and Swanson, 1996], and at the watershed scale [Wondzell et al., 2010]. These fluctuations make the extent of the hyporheic zone dynamic and even more challenging to define. Determining ways to quantify the extent of the hyporheic zone has been and continues to be the subject of much previous research [Brunke and Gonser, 1997; Cardenas, 2009; Cardenas and Wilson, 2007b; White, 1993]. While the effects of tidal fluctuations have been understood in coastal settings [Li and Jiao, 2003; Nielsen, 1990; Rotzoll et al., 2008], similar detailed scrutiny is needed in larger rivers to better understand the function of the hyporheic zone in rivers that represent the majority of our waterways in size and prevalence of anthropogenic impacts.

[6] The hyporheic zone provides connectivity between surface water and groundwater, and is the locus of many biogeochemical reactions [Boulton et al., 1998]. The importance of the hyporheic zone is controlled primarily by hydraulic processes [Bencala, 2005; Findlay, 1995; Hancock, 2002]. These water exchanges occur at multiple spatial and time scales [Cardenas, 2008] and have the potential to impact both river and groundwater chemistry and temperature [Brunke and Gonser, 1997; Hester et al., 2009; Swanson and Cardenas, 2010]. The exchanges that occur in the hyporheic zone affect both surface and groundwater systems; upwelling water introduces nutrients to the river system, while percolating water provides organic matter and dissolved oxygen to organisms that act as a “biological filter” in the hyporheic zone. The direction of exchange determines which biogeochemical processes occur in the hyporheic zone and at what rate; these exchange processes are mediated by the hydraulic gradient between the river and the streambed.

[7] The hyporheic zone offers protection to organisms in all life stages including fish embryos, insect eggs and pupae, and other larvae and invertebrates. The haven of the saturated sediments prevents organisms from being washed away during high flows, dried out during low flows, and also protects them from extreme temperature fluctuations [Brunke and Gonser, 1997]. The importance of the hyporheic zone to some species of salmonids is well documented; the spawning and incubation of the eggs require the buffered temperatures and high concentrations of dissolved oxygen that are created in natural hyporheic zones [Findlay, 1995; Malcolm et al., 2004; Shepherd et al., 1986]. While natural fluctuations are necessary for the health of the hyporheic ecotone, Curry et al. [1994] described the negative impacts of river regulation on the trout spawning and incubation that occurred in the hyporheic zone of a Canadian river. Calles et al. [2007] also observed dissolved oxygen levels in a regulated river in Sweden that fell below the minimum requirements of the incubation of brown trout embryos. A complete

understanding of the hyporheic zone hydraulic response to large, regular stage fluctuations will lead to a full understanding of the corresponding effects on the hyporheic zone as a habitat.

[8] Hyporheic zone temperatures are controlled by the magnitude of surface water-groundwater exchange. While groundwater temperatures fluctuate minimally, river temperatures often experience diel fluctuations of several °C. In a base flow-dominated system, hyporheic zone temperatures remain nearly constant on a daily scale, and vary with changes in groundwater temperature over longer annual scales [Constantz, 2008]. In a system where the stream recharges the aquifer, the streambed can experience daily fluctuations in temperature that are attenuated and delayed with distance and depth from the surface water body [Cardenas and Wilson, 2007c, 2007d; Swanson and Cardenas, 2010]. The streambed temperature regime can affect biogeochemical processes, microbial activity, and invertebrate development [Ward and Stanford, 1982]. Hanrahan [2008] showed the critical nature of streambed temperatures to the successful incubation and emergence of salmonids.

[9] Previous research has implied that regular dam releases impact the size and significance of the hyporheic zone [Hancock, 2002; Nilsson and Berggren, 2000; Winter et al., 1998], but only a few have presented observations of regulated systems [Arntzen et al., 2006; Boutt and Fleming, 2009; Sawyer et al., 2009]. While Arntzen et al. [2006] focused their measurements within the streambed, Boutt and Fleming [2009] and Sawyer et al. [2009] focused on the riparian aquifer within the banks. All three studies show that river stage fluctuations pump river water in and out of the surrounding sediment with implications for temperatures and chemistry. However, the timing and magnitudes of the exchange flows are expected to vary between the riparian aquifer where bank storage dominates and the channel bed where the hydrologic response is nearly instantaneous. Here, we combine high-resolution measurements of head and temperature along a riparian-to-hyporheic transect and show that exchange flows are greatest along the channel margins and diminish toward the channel centerline. Additionally, the variation in timing between exchange flows in the channel and banks may create spiraling flow paths that impact the transport of nutrients and contaminants.

## 2.2. Study Site

[10] The lower Colorado River (LCR), which flows through Austin, Texas (USA), is an ideal site to study the impacts of river regulation as there are more than ten regulating dams on the LCR. Our field site in the LCR is located at Hornsby Bend, 10 km southeast of downtown Austin and 23 km downstream from the Tom Miller Dam, which regulates the river for hydropower generation (17 MW capacity) (Figure 1). At Hornsby Bend, the LCR is approximately 65 m wide and the mean depth is 1.3 m. The streambed is composed mainly of alluvial deposits, and the river bank adjacent to our instrument transect is nearly vertical. The effects of river regulation on water table dynamics in the bank of the LCR were previously studied by Sawyer et al. [2009], while Francis et al. [2010] mapped dynamic water tables across a large gravel island in the LCR.

[11] The USGS stream gauge site 08158000 is located approximately 12 km upstream of Hornsby Bend. At this

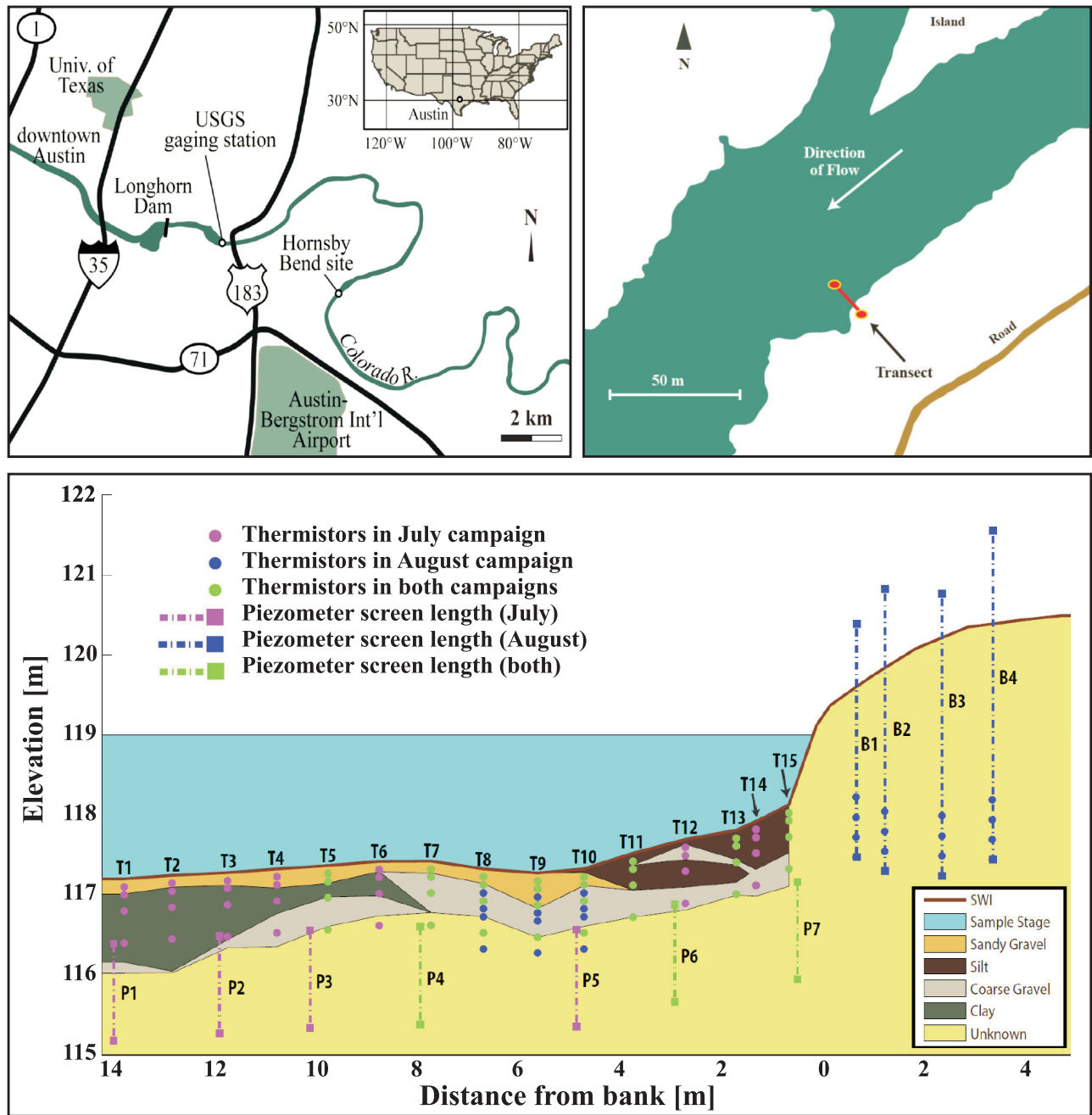


**Figure 1.** (top) Location of the field site, Hornsby Bend, on the Colorado River in relation to Austin, Texas landmarks and location of transect instrumented at Hornsby Bend (modified from Sawyer *et al.* [2009]). (bottom) Interpreted sediment distribution at the study transect estimated by probing with rebar to a maximum depth of 1.2 m, and placement of instrumentation in both field campaigns. The beige-colored “Unknown” sediments are most likely similar alluvial deposits.

gauge, the contributing drainage area to the LCR is approximately 71,500 km<sup>2</sup>. The gauge datum is approximately 123 m above sea level. The daily mean discharge for data collected between 1898 and 2010 is 68.4 m<sup>3</sup>/s. This is equivalent to a mean annual discharge of 2.16 × 10<sup>9</sup> m<sup>3</sup> per year. From 7 July to 7 August of 2009, encompassing the period of our field studies, the mean daily discharge was 37.0 m<sup>3</sup>/s. Maximum mean daily discharge was 99.5 m<sup>3</sup>/s and minimum daily discharge was 2.2 m<sup>3</sup>/s over the same period.

[12] During the summer of 2009, daily releases from the Tom Miller Dam were timed to allow for peak hydroelectric power generation. Regulation by the Tom Miller Dam causes daily stage fluctuations of approximately 1.5 m at the field site (Figure 2). The dynamics at this field site merit detailed observation as the impacts of the fluctuations are extensive both for kilometers downstream but also laterally into the riparian zone. On average, the LCR is a regionally gaining river, but the regular stage fluctuations cause

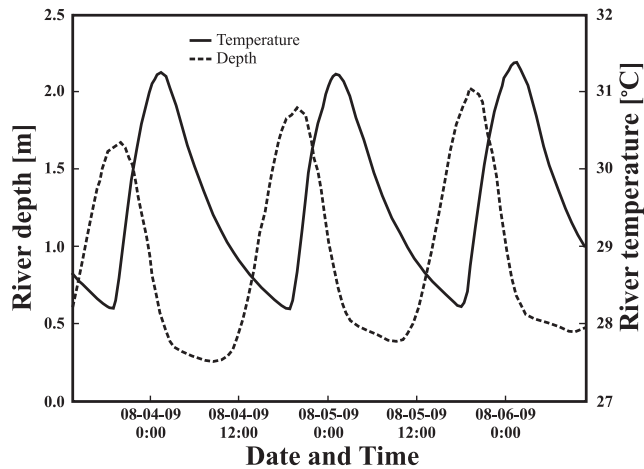


**Figure 2.** Observed asynchrony between river stage and temperature measured at Hornsby Bend over multiple 24 h cycles. Stage varies by 1.5 m with a mean depth of 1.3 m and temperature varies by approximately 3 °C each day.

portions of the river to both gain and lose within each 24 h cycle at Hornsby Bend.

### 3. Methods

[13] Two field campaigns were conducted to measure pressure and temperature at high temporal and spatial resolution over multiple regulation cycles in both the streambed and bank. Heat is used as a tracer to determine the extent and variability of surface water-groundwater exchange through monitoring of the temperature signals observed in the river and at multiple depths in the streambed. The rate of infiltration of river water into the streambed is reflected by the penetration of a river's thermal signal into the streambed [Constantz, 2008; Hatch et al., 2006; Swanson and Cardenas, 2010]. Hydraulic head data, combined with hydraulic properties of the bank and streambed, are used to quantify the spatial variation of fluid fluxes in the streambed and water table fluctuations in the adjacent bank.

#### 3.1. Monitoring Methods

[14] Pressure and temperature sensors were installed in the LCR, its streambed, and adjacent bank to monitor conditions for two three-day periods during the summer of 2009 (Figure 1). Between 7 and 10 July, a transect of 15 vertical thermistor arrays (each consisting of four HOBO TMC thermistors connected to a U12 data logger), spaced 1 m apart laterally, recorded temperature in the streambed. In each of the 15 vertical profiles, thermistors installed at 10, 20, 40, and 80 cm below the sediment-water interface (SWI) recorded streambed temperature every 5 min (Figure 1). The thermistors were suspended inside a 2.5 cm diameter steel pipe that had a drive point at its tip. Steel pipes with this small diameter thermally equilibrate quickly, ~8–10 min, with their surroundings [Cardenas, 2010]. These steel pipes extended above the maximum river stage and were only open at the top. Six PVC piezometers and one river-stage recorder were also installed in the channel to monitor vertical head gradients. These piezometers were spaced approximately 2 m apart in the transect. The PVC piezometers had a 3.8 cm inside diameter and were 13.8, 11.7, 9.9,

4.7, 2.8, and 0.4 m from the mean shoreline (Figure 1). Piezometers in the streambed had a screen interval of 1.22 m with the top of each screen located 0.8 m below the SWI (Figure 1). In situ Aqua Troll 200 probes inside the piezometers measured water level every 15 min. Similarly, river stage and temperature were monitored every 15 min using an Aqua Troll 200 probe.

[15] In the measurement campaign of 3 to 6 August, four bank piezometers were added to the transect at distances of 0.8, 1.4, 2.5, and 3.5 m inland of the riverbank to monitor lateral hyporheic exchange (Figure 1). These piezometers were screened through the land surface, far above the maximum water table. In situ Aqua Troll 200 probes deployed in the piezometers recorded the water level every 10 min. In order to gain higher spatial resolution of the thermal dynamics than in the first campaign, three detailed vertical arrays were deployed at points T8, T9, and T10 (Figure 1), in the area of the streambed composed of sandy/gravel sediments (high permeability). Each array had eight thermistors located at 10, 20, 30, 40, 50, 60, 80, and 100 cm below the SWI. Five vertical temperature arrays were deployed in the streambed as in the first campaign at T5, T7, T11, T13, and T15 with thermistors vertically located at 10, 20, 40, and 80 cm below the SWI (Figure 1). All thermistors recorded temperature every 5 min as in the first campaign. Pressure transducers were also deployed in three of the streambed piezometers used in the first campaign (P4, P6, and P7), with the top of each screen 0.8 m below the SWI (Figure 1). A river stage recorder (also an Aqua Troll 200 probe) was used to measure river depth and temperature every 10 min as before.

[16] The elevations of the SWI, adjacent bank topography, and top-of-casing for each piezometer and vertical thermistor array were surveyed relative to previously used benchmarks using a Sokkia total station which is accurate to <1 mm.

#### 3.2. Streambed Lithologic and Hydraulic Characterization

[17] The lithology of the streambed was estimated by probing with a steel rod (a manual version of a penetrometer) to a maximum depth of 1.2 m below the SWI. At the transect, the streambed has areas of silt, clay, sandy gravel, and coarse gravel (Figure 1). At the bank, a 0.5 m thick layer of silt covers the surface of the streambed, beneath which is coarse gravel. In the center of the transect, the surface of the streambed is sandy gravel which extends to a layer of coarse gravel. Near the center of the channel, a 0.15 m thick layer of sandy gravel comprises the streambed surface. Below this sandy gravel layer are deposits of clay that extend beyond the maximum probing depth of the rebar.

[18] In-stream pneumatic slug tests were completed in the streambed at depths of 15, 40, and 80 cm, adjacent to piezometers located in sand and gravel sediments to determine their hydraulic conductivity ( $K$ ). The slug tests apparatus consisted of a 3.2 cm diameter steel piezometer with a 20 cm screen and an in situ Level Troll 700 pressure transducer suspended inside. The piezometer was driven into the streambed, sealed, and pressurized. A volume of air was added (pushing water out of the piezometer) using a bicycle pump. The seal on the piezometer was then released and the transducer monitored the recovery of the

water level in the well every 0.25 s. This technique is described in full detail by *Cardenas and Zlotnik* [2003].

[19] Hydraulic conductivity values ranged from 10 to 50 m/d. However, we were unable to make slug test measurements in the areas of high clay (at the river midline) and silt (at the bank) because of clogging of the piezometer screen. To determine a representative value of vertical  $K$  for the entire transect,  $K$  values were first averaged vertically for each piezometer location using the harmonic mean. The resulting average vertical  $K$  values at each piezometer location were then averaged across the transect using the arithmetic mean. Local isotropy over the support volume of the slug test is assumed. The final value of 15.7 m/d is considered as representative of the vertical  $K$  at the transect but is biased toward the shallower more permeable sediments.

### 3.3. Analysis Methods

[20] Measurements of hydraulic conductivity and hydraulic gradients were used to estimate vertical fluxes, hydraulic depth of the hyporheic zone, and exchange times. The impacts on the water table in the river bank were also analyzed. Temperatures measured in the river and at multiple depths in the streambed were used to estimate the thermal depth of the hyporheic zone as well as to trace the movement of water in the streambed.

[21] Instantaneous vertical fluid fluxes are calculated following the Darcy equation:

$$q(x, t) = -K \frac{\partial h(t)}{\partial z}, \quad (1)$$

where  $q$  is the Darcy flux,  $h$  is hydraulic head, and  $\partial h / \partial z$  is the vertical head gradient. The calculated  $q$  is used to estimate the depth of the hyporheic zone throughout the transect. This depth was calculated as the integration of the pore water velocity ( $v = q / \phi$ , where  $\phi$  is porosity set at 0.3) during the time of downward-flow, between  $\tau_1$  and  $\tau_2$  when the vertical flux is negative:

$$Z_{HZ}(x) = \int_{\tau_1}^{\tau_2} v(x, t) dt. \quad (2)$$

[22] The time interval from  $\tau_1$  to  $\tau_2$  is the time when the river is losing and the integration is numerical. Essentially, this is particle tracing to determine the maximum penetration depth of river water into the streambed. Three periods of negative flux were analyzed, and the penetration depths estimated at each piezometer were averaged over the three days.

[23] The estimated penetration depths of river water into the streambed were used to estimate a hyporheic exchange time. This exchange time is calculated as

$$T_{HZ}(x) = (\tau_2 - \tau_1) + \int_{-Z_{HZ}}^0 \frac{dz}{v(x, t)}, \quad (3)$$

where  $(\tau_2 - \tau_1)$  is the time interval during which the river is losing. The second term in equation (3) represents the time it would take a water parcel to return from the point of

deepest penetration where  $v$  is positive (implying upward groundwater flow).

[24] To determine the extent of regulation impacts on the riparian zone, the amplitude of the water table fluctuations measured in the bank are compared to the fluctuations in river stage. The water table response to sinusoidal stage fluctuations is expected to be exponential in shape based on the analytical model of aquifer head response shown in *Singh* [2004]. Accordingly, the penetration of water table fluctuations into the adjacent bank is estimated using an exponential fit to the amplitudes measured in the four bank piezometers. This fit is extended into the aquifer to determine where the amplitude of the water table fluctuations in the bank has attenuated to 10% of the river stage fluctuations. This point is taken to be the limit for the most significant impacts on the bank's water table.

[25] The thermal properties of the streambed at the base of each piezometer were determined using a Decagon KD2 Thermal Properties Sensor with probes that measure thermal conductivity, heat capacity, and thermal diffusivity. Values of thermal conductivity ranged between 0.80 and 2.3 W/(m · K), with a mean value of 1.7 W/(m · K). Values of volumetric heat capacity ranged from 2.4 to 3.7 MJ/(m<sup>3</sup> · K), with a mean value of 3.0 MJ/(m<sup>3</sup> · K). Values of thermal diffusivity ranged from 0.24 to 0.89 mm<sup>2</sup>/s, with a mean value of 0.61 mm<sup>2</sup>/s. These thermal properties provide site-specific estimates of properties that dictate how the thermal wave from the river penetrates into the streambed.

[26] The thermal damping depth characterizes how far a sinusoidal thermal signal penetrates into the streambed if pure conduction drives the penetration. At the damping depth, the predicted amplitude is 37% of the forcing thermal signal. This depth  $d$  is calculated from the streambed physical properties and the frequency of the signal via

$$d = \sqrt{\frac{K_T T}{\pi}}, \quad (4)$$

where  $K_T$  is the thermal diffusivity of the streambed and  $T$  is the period of the wave. For the Hornsby Bend site with  $K_T = 0.61$  mm<sup>2</sup>/s and  $T = 1$  day, the  $d = 13.0$  cm. Even with the maximum observed value of thermal diffusivity,  $K_T = 0.89$  mm<sup>2</sup>/s, the  $d$  is only 15.6 cm. A thermal signal that propagates deeper than the damping depth into the streambed indicates that advection is an important transport mechanism.

## 4. Results

### 4.1. River Stage Fluctuations

[27] During both field campaigns, the LCR at Hornsby Bend had a mean depth of 1.3 m with a daily fluctuation of 1.5 m (Figure 2). The maximum river stage of 2.1 m occurred at approximately 01:30 in the early morning. Minimum river stage, 0.6 m, occurred 17 h later at 18:30 each day. The rising limb of the stage fluctuations took place over 7 h, while the falling limb occurred much more gradually over 17 h (Figure 2).

### 4.2. Hydraulic Gradients, Fluxes, and Exchange Times

[28] The observed head gradients and average hydraulic conductivity were used to calculate the daily average or net

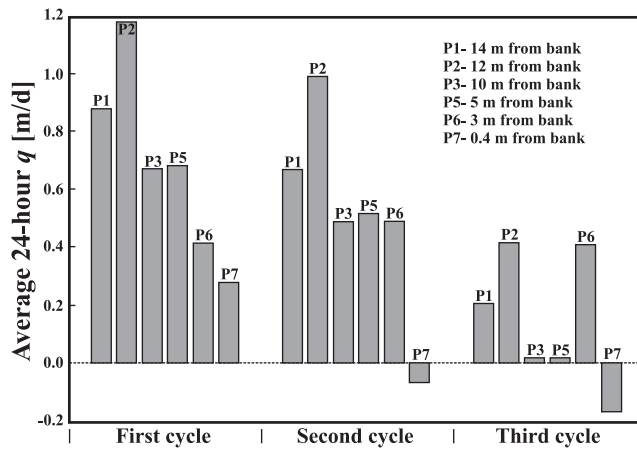


**Figure 3.** The average vertical flux over each 24 h cycle observed at each piezometer. P1 is the piezometer nearest to the middle of the river, while P7 is the piezometer closest to the bank. Average flux near the center of the river is always positive, while the average flux near the bank can be close to zero or negative.

fluid fluxes over three 24 h cycles at Hornsby Bend. Positive fluxes indicate net upwelling flow into the river (the river is gaining), whereas negative values indicate net flow from the river (the river is losing). The largest average daily fluxes occurred at the piezometers nearest the channel midline away from the bank (Figure 3). The average daily flux at P1, the piezometer nearest the river midline, was estimated to be 0.60 m/d (gaining) over three days of observation. Daily net flux declines with proximity to the bank, and small positive and even some negative average daily fluxes occurred at the piezometers nearest the bank (Figure 3). The average daily flux at P7, the piezometer closest to the bank, was estimated to be 0.01 m/d over one three-day field campaign. While the center of the river is primarily gaining, the daily net fluxes at the edge of the channel are closer to neutral.

[29] These fluxes are used to estimate the vertical extent of the hyporheic zone throughout the transect. The estimated penetration depth of the river water into the streambed is more than 3.5 m at the bank, while only 0.5 m at the middle of the channel (Figure 4). These results are consistent with previous modeling that predicts upwelling groundwater acts to limit the depth of hyporheic pumping [Boano *et al.*, 2008; Cardenas and Wilson, 2007a]. As the extent of the hyporheic zone is much shallower near the river midline, the exchange time is also much smaller than at the bank (Figure 4). Near the channel midline, river water requires 12 to 15 h to exchange through the full hyporheic zone. The distribution of exchange times in the streambed increases to longer times at the bank where the exchange time is nearly 24 h.

[30] When the river stage is low, during late morning and afternoon, groundwater discharges to the river. Data from the piezometers installed in the streambed indicate a potentiometric surface above the river stage during this time (Figure 5 and Movie S1 in the auxiliary material).<sup>1</sup> When the

<sup>1</sup>Auxiliary materials are available in the HTML. doi:10.1029/2010WR009794.

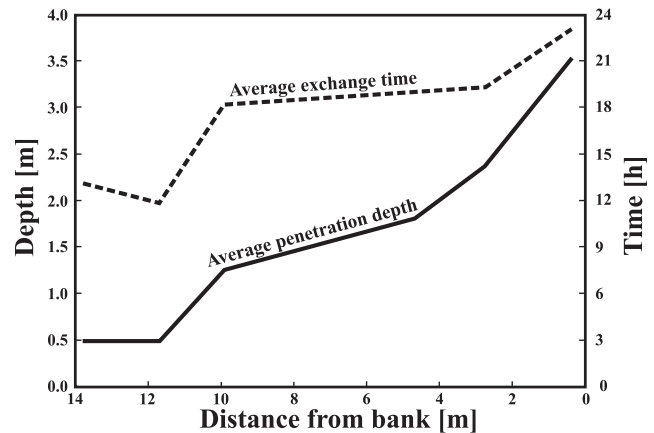


**Figure 4.** Depth of the hyporheic zone and exchange time calculated using vertical exchange fluxes. With increased proximity to the bank, both the extent of the hyporheic zone and the exchange time increases.

river stage is at its maximum during the night, the river recharges the surrounding riparian aquifer.

[31] Instantaneous vertical fluxes through the streambed vary both as a function of time and distance from the bank (Figure 5). When the river stage is at its minimum, estimated instantaneous vertical fluxes range between +2.2 and +3.2 m/d up through the streambed (gaining river) with fluxes at the bank higher than those toward the middle of the river. When the river stage is at its maximum and when the river is losing water, a flux of  $-3.0$  m/d occurs adjacent to the bank, while at the center of the river vertical flux is only  $-0.5$  m/d. Between these extremes, there are times when part of the transect is gaining and part of the transect is losing. The variability in instantaneous flux over a 24 h period is much greater at the bank (between +3.2 and  $-3.2$  m/d). This is consistent with the estimated daily average fluxes at the bank, which are close to neutral. Toward the middle of the river, instantaneous flux is more often positive (gaining) than negative (losing), ranging between +2.2 and  $-0.5$  m/d.

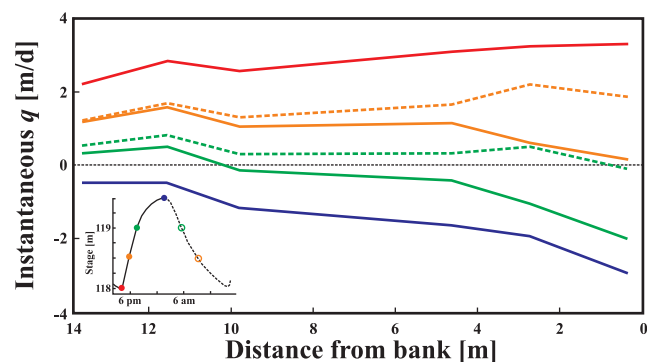


**Figure 5.** Spatiotemporal variation of instantaneous flux across the transect. When the river is at its lowest stage (red), the entire transect is gaining. When at maximum stage (purple), the entire transect is losing. The greatest variability in flux occurs at the bank. The inner framed key shows river stage over 1 day. Points indicate times when vertical fluxes are plotted in the graph. Solid lines represent rising stage while dashed lines represent falling stage.

During minimum river stage when the river is strongly gaining from base flow, the instantaneous vertical flux is largest near the bank and becomes smaller toward the river midline. This is consistent with flux patterns suggested by the theoretical model of *Boano et al.* [2008].

### 4.3. Hysteresis in Head Gradients

[32] In all piezometers, the hydraulic head rises and falls over the course of a day, driven by the stream stage. In three piezometers (P1, P2, and P3), the vertical head difference between the bed and river depends on stream stage, but not on whether stage is rising or falling. These piezometers are located 14, 12, and 10 m from the bank, respectively (Figure 1). Closer to the bank, however, the vertical head difference depends not only on stream stage but also on whether stage is rising or falling, indicating a hysteretic relationship between head gradient and stream stage. Hysteresis is maximum in the piezometer closest to the bank (P7, 0.4 m from the bank) and decreases as one moves away from the bank. Figure 6 presents the hysteretic relationship observed in P7, along with the one-to-one relationship seen in P3. At P7, the response of the potentiometric surface appears to lag the stream stage fluctuations by 30 min.

### 4.4. Bank Water Table Fluctuations

[33] A second field campaign was implemented to measure water table elevation in the adjacent bank simultaneously with monitoring in the streambed. Water table fluctuations were monitored at four piezometers in the adjacent bank, 0.8, 1.3, 2.5, and 3.5 m inland, respectively (Figure 1). The impacts of river-stage fluctuations on the water table are attenuated and delayed with increasing distance into the bank (Figure 7 and Movie S1 in the auxiliary material). Near maximum stage, the river intersects the piezometer screen exposed above the land surface of the nearest bank piezometer. Peak water table elevation was delayed 0, 20, 60, and 90 min in order of increasing distance inland. Greater lag times are seen during the falling limb of the

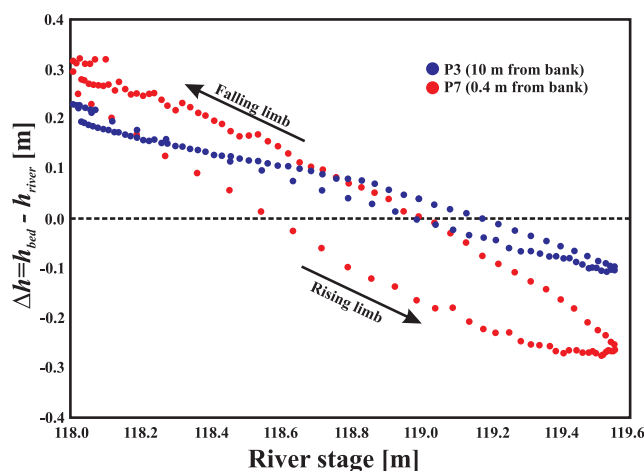


**Figure 6.** Head difference  $\Delta h$  between a streambed piezometer and the river plotted against river stage through a 24 h cycle. The relationship at P3, a piezometer 10 m from the bank, shows no hysteresis. While at P7, the piezometer located only 0.4 m from the bank, shows significant hysteresis. See Figure 1 for location of piezometers.

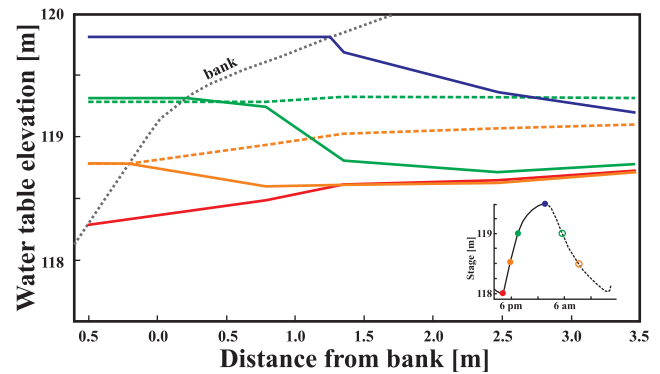


**Figure 7.** Bank water table profiles. The envelope of fluctuations implies that transient bank storage is at work and in fact may cause the hysteresis in streambed instantaneous flux near the bank (Figure 5).

water table fluctuations than during the rising limb (indicating another hysteretic response in the bank). The minimum water table elevation was delayed 30, 60, 90, and 100 min. The amplitudes of the water table fluctuations are 88%, 75%, 57%, and 47% of the river-stage amplitude as one moves away from the river. An exponential fit to the amplitude of the water table fluctuations with distance inland indicates that the fluctuations decay to 10% of the river-stage amplitude fluctuations 10 m inland of the mean shoreline.

### 4.5. Temperature Distribution

[34] River temperature fluctuated over diel cycles with an amplitude of approximately  $3.5^{\circ}\text{C}$ . Maximum temperature occurred in the early evening,  $31.0^{\circ}\text{C}$  at 19:30, and minimum temperature occurred in the early morning,  $27.5^{\circ}\text{C}$  at 08:00 (Figure 2). Data collected from the 60 thermistors in the streambed during the July field campaign demonstrate the propagation of the river's temperature into the streambed to a depth of at least 1 m (Figure 8 and Movie S2 in the auxiliary material). Maximum penetration is seen in the highest permeability area of the streambed, between thermistor arrays T8 and T10, where the streambed is mainly sand and gravel (Figures 1 and 8). Before the hydraulic gradient reversal, the maximum temperature  $\sim 10$  cm below the SWI occurs near maximum river stage when downward flow is the strongest (Figure 9). The maximum depth of thermal signal penetration occurs soon after the hydraulic gradient reversal.

[35] At T10 (and the vertical arrays that similarly experienced high penetration of the thermal signal), the peak daily temperature 10 cm below the SWI occurred 4 h after the maximum river temperature (Figure 9). The amplitude of temperature fluctuations 0.5 m below the SWI is  $0.6^{\circ}\text{C}$ , or 20% of the daily river temperature fluctuation amplitude. One meter below the SWI, the peak daily temperature is shifted 12 h after the peak in river temperature. The amplitude of the temperature fluctuations 1 m below the SWI was attenuated to  $0.3^{\circ}\text{C}$ , or 12% of the daily river temperature fluctuation amplitude.

[36] When the river stage is at its minimum, groundwater discharge to the river prevents the warm river water from penetrating into the streambed (Figures 8 and 9 and Movie S2 in the auxiliary material). Even though the river temperature is several degrees warmer when the river is gaining

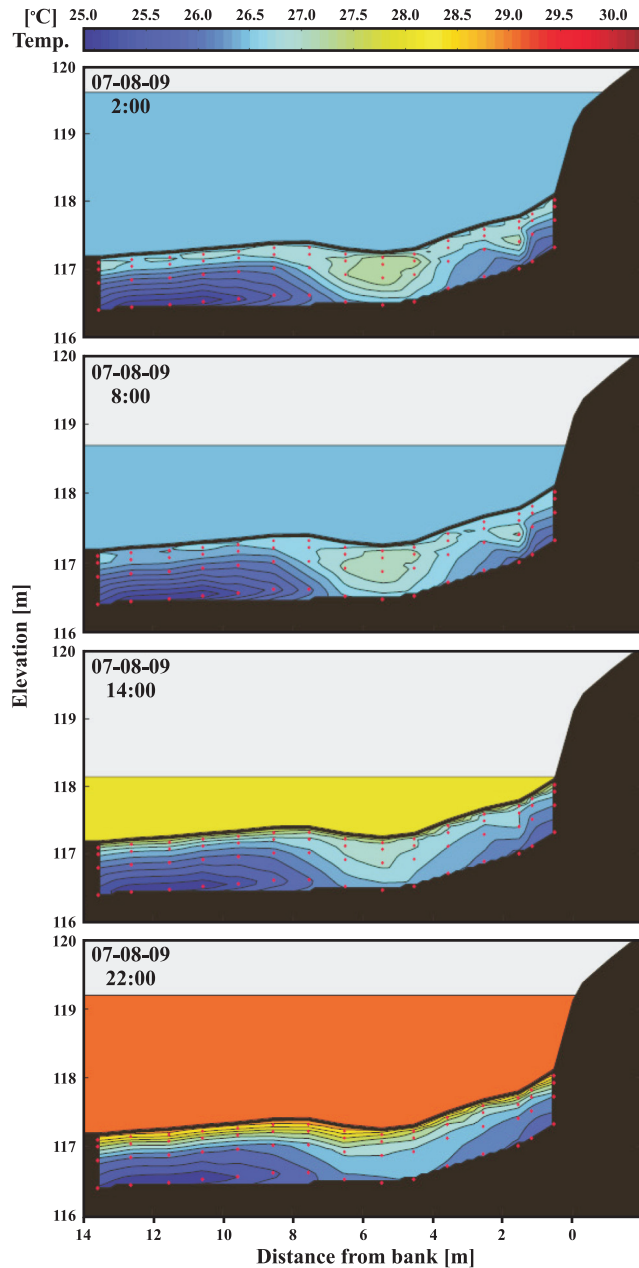


**Figure 8.** Temperatures in both the river and streambed. During low stage, the river's temperature signal penetrates deeper into the streambed. During upwelling, the temperature signal is confined to the uppermost 10 cm of the streambed.

than when it is losing, the upwelling limits the penetration of the river's temperature signal to the upper 10 cm below the SWI (Figures 8 and 9). This limit on the penetration of the temperature signal is consistent throughout the river transect, regardless of the permeability of the sediment where the thermistors are deployed.

## 5. Discussion

[37] A few simplifications allow for intuitive interpretations of the data. First, the value of hydraulic conductivity chosen for calculating the Darcy fluxes is the average value

of hydraulic conductivity observed in the transect during slug tests. This value does not reflect the full heterogeneity of the streambed sediments in the transect, which range from fine clay and silt to coarse gravel. Moreover, the monitoring follows a 2-D transect perpendicular to the channel. Processes may be occurring in 3-D. Also, when estimating the pore velocity used to calculate the depth of the hyporheic zone and the exchange times, we assumed uniform streambed porosity. Even with these simplifications, these data allow for further insight into the connection between hyporheic response in the streambed and bank, particularly with regular stage fluctuations.

### 5.1. Altered Hydraulic Processes

[38] In an unregulated, base flow dominated river system, the vertical extent of the hyporheic zone would be limited by upwelling groundwater [Boano *et al.*, 2008; Cardenas and Wilson, 2007a]. At Hornsby Bend, water is pumped in and out of the hyporheic and riparian zones on a daily cycle because of dam releases. Large stage fluctuations generate large hydraulic gradients and enhanced mixing, increasing the importance of the hyporheic zone in a regulated river system. These releases extend the depth of the hyporheic zone, as shown in both the analyses of the collected streambed hydraulic and temperature data (Figures 5, 8, and 9). Moreover, in a base flow dominated river, one would expect the average daily flux to be positive throughout the transect. Regulation in the LCR causes the net daily fluid fluxes near the bank to be closer to neutral (Figure 3).

[39] Average flux across the transect varies from one day to another (Figure 3). These changes may be because of the small changes in the timing and amplitude of the stage fluctuations from day to day. There were slight differences in the maximum, minimum, and mean river stage and timing throughout both periods of observation (Figure 2). The amplitudes of the stage fluctuations for each cycle in Figure 3 are 1.56, 1.53, and 1.58 m, respectively. Even though these are small differences of a few centimeters, this variation may cause significant differences in average flux seen at the same position from day to day. Other hydrologic factors, such as recharge from a previous rain event outside of the measurement period (there was no precipitation during the experiments) or different evapotranspiration rates from the riparian zone, may also have had an effect on the daily regional groundwater flow toward the river, altering the observed net fluxes.

[40] Through each 24 h cycle, the river transitions from gaining when the river stage is low to losing when the river stage is high. For two periods of time each day (during the rising and falling limbs of the release floods), part of the transect is gaining while another section is losing (Figure 5, green lines). These reversals in hydraulic gradient vary both temporally and spatially across the river transect; they highlight the multidimensional nature of the flow paths. This multidimensionality has been studied through numerical modeling experiments [Desilets *et al.*, 2008; McCallum *et al.*, 2010] which in fact suggested that these dynamic flow paths be investigated using field studies.

[41] Greater magnitudes and variability in exchange were consistently measured closer to the bank. Toward the middle of the channel, the instantaneous flux is predominantly out of the streambed. This discharge into the river

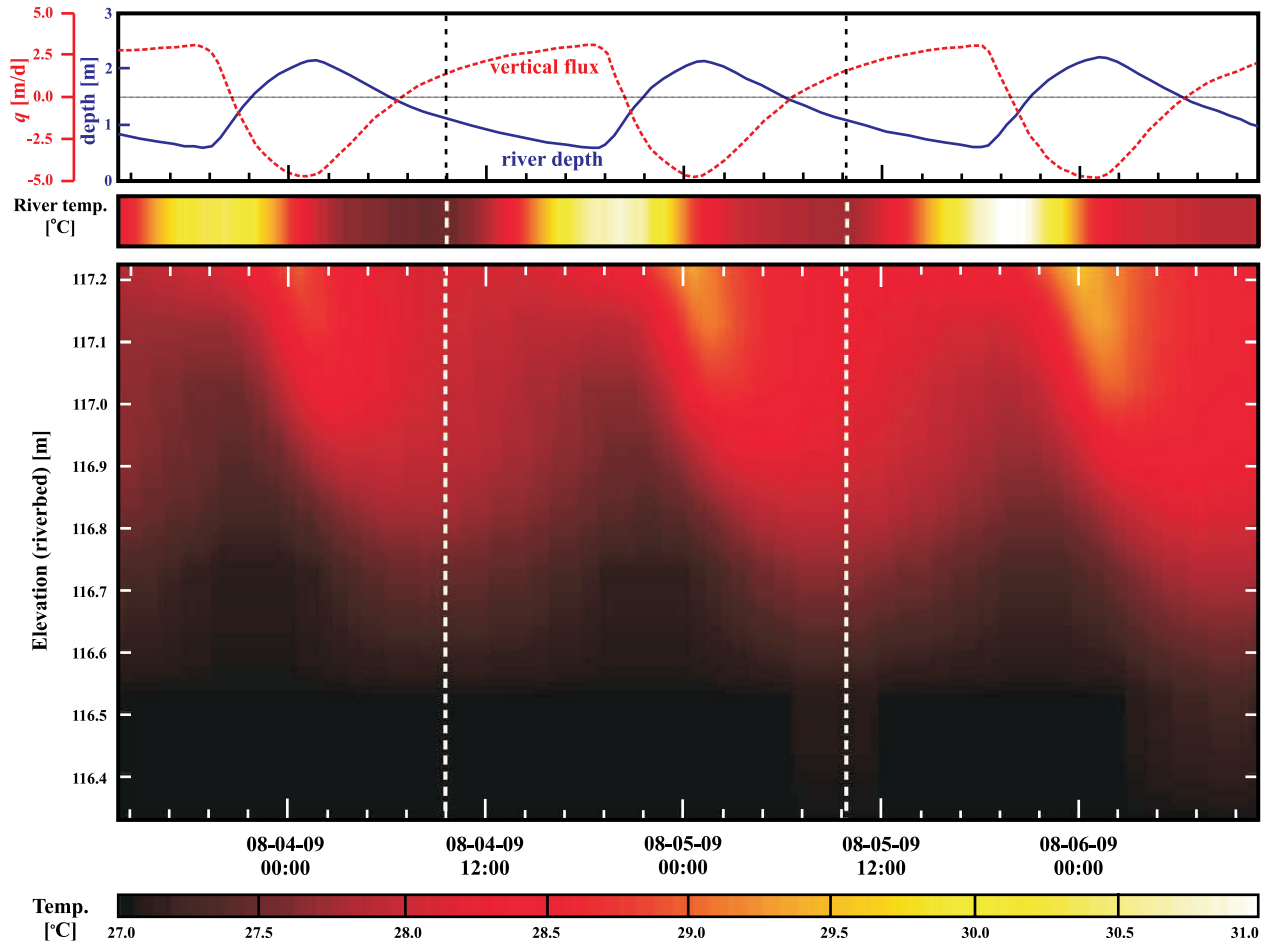


**Figure 9.** Streambed temperature, river temperature, river stage, and instantaneous vertical fluid flux through time at profile T10 in the transect (see Figure 1 for location). Positive flux indicates upwelling, while negative flux is downwelling. The top of the streambed temperature plot corresponds to the sediment-water interface.

prevents the hyporheic zone from extending any deeper. Also, with increased distance from the bank, the instantaneous fluxes at a specific stage elevation are nearly equal for both the rising (solid line) and falling (dashed line) limbs of the stage fluctuations (Figure 5, green and orange lines). At the bank, the instantaneous flux at a specific stage elevation differ by up to  $\sim 2$  m/d depending on whether the stage is rising or falling. When the stage is at an elevation of 119.0 m (Figures 5 and 7, green lines), the flux is neutral ( $\sim 0$  m/d) at the bank when this is a falling stage (dashed green line), but is strongly downward ( $\sim -2$  m/d) when the stage is rising (solid green line).

## 5.2. Hysteresis and Connections Between the Streambed and Bank Hyporheic Zones

[42] A hysteretic response occurs in the water table fluctuations monitored in the bank (Figure 7). The water table elevation corresponding to a specific river stage is significantly different depending on whether the stage is rising or falling. For example, at 1.5 m into the bank, when the river stage is approximately 118.75 m (Figure 7, orange lines), the water table elevation is either 118.6 m (when the stage is rising) or 119.0 m (when the stage is falling). This hysteresis in the bank drives hysteresis seen in the adjacent

streambed (Figure 6). Water is stored and released from the bank which impacts gradients along the outer margins of the streambed.

[43] The hysteretic responses indicate a hydraulic connection with transient bank storage driving the hysteresis seen in both the streambed and bank. We surmise that there is an area where this hydraulic connection is most significant (perhaps a few meters from the shoreline on each side) (Figure 10). Within this near-bank zone, bank storage buffers the water table response to falling river stage. Effects because of nonlinear processes in the vadose zone such as hysteresis in wetting and drying cycles and capillarity effects are integrated into this. These effects propagate through the hydraulic gradient response in the streambed where water stored in the bank is released rapidly through the streambed as river stage falls, creating a fast gradient reversal from a losing river to a gaining river. There may also be a transition zone where transient bank storage may affect the head gradients in the streambed, though less significantly. Outside of these zones, the response in the bank is attenuated significantly and the response in the streambed is in phase with the river stage. *Arntzen et al.* [2006] hypothesized that along-channel variance in the magnitude and hysteresis in the streambed hydraulic gradient may correspond to the permeability of

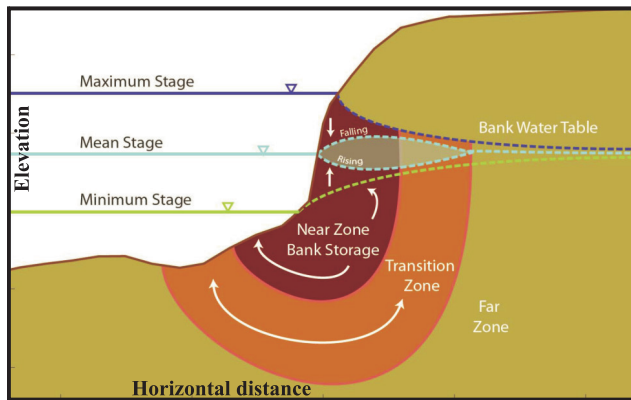


**Figure 10.** Conceptual illustration of effects of transient bank storage on hyporheic processes in the streambed adjacent to the bank. Transient bank storage is suggested as the cause for the hysteretic response seen in streambed fluxes at the bank. With increasing distance into the bank, this envelope of high impact bank storage dissipates.

bed sediments. Similarly, at our site, the size of this near-stream zone where a strong hysteretic relationship exists should be dependent not only on the properties of the streambed sediments but also of the bank material.

[44] Hysteresis in instantaneous flux is greatest near the bank (Figure 5) and appears in three piezometers closest to the bank (the furthest being 5 m from the mean shoreline). In this near-bank zone, bank storage impacts the vertical fluxes observed in the streambed. With rising river stage, the hydraulic gradient reversal farther from the bank takes longer to occur. At the bank, the added storage volume as well as the bank water table fluctuations may increase the hydraulic gradient such that downwelling occurs more rapidly and more strongly. When the river stage is falling, the hysteresis of the bank water table fluctuations may similarly create a stronger hydraulic gradient in the streambed near the bank such that more water upwells into the river. *McCallum et al.* [2010] modeled hysteresis in total flux between a partially penetrating river and its adjacent bed and bank. In their modeling study, the river is base flow fed and undergoes flooding so this is directly analogous to the LCR. However, the fluxes we presented here are only vertical fluxes while they show total fluxes (across the bed and saturated bank). It is more appropriate to compare total flux time series presented by *Sawyer et al.* [2009] who studied a bank transect on the LCR just a few meters away from where this study was conducted. The calculated temporal patterns in fluxes in Figure 9 of *Sawyer et al.* [2009] are in fact very similar to those in Figure 6 of *McCallum et al.* [2010] where they attribute this to bank storage, a phenomenon which is explicitly considered in their unsaturated flow model. The hysteresis in flow paths and fluxes suggest that a parcel of water going into the bed and bank does not necessarily follow the same path going back. This may have implications on biogeochemical processes and patterns.

### 5.3. Thermal Processes

[45] During losing periods, dam operations strongly influence streambed temperatures, allowing the river's warmer temperature signal to penetrate at least a meter into the bed (Figure 9). One meter below the SWI, the streambed tem-

peratures fluctuate  $0.3\text{ }^{\circ}\text{C}$  daily and lag river fluctuations by 12 h. In an unregulated, base flow-dominated river system, the discharge of groundwater to the river would keep streambed temperatures constant even only a few centimeters below the SWI [*Cardenas and Wilson, 2007c*]. According to a theoretical calculation of the damping depth (or  $e$ -folding depth) of a penetrating periodic thermal signal, the amplitude of the streambed temperatures should only be 37% of the river's temperature fluctuations at 13 cm below the SWI. In the LCR, a decay to 37% of the river's amplitude was not observed until nearly 30 cm below the SWI. Moreover, at a depth of 1 m, the theoretical model predicts that the streambed temperature fluctuations should only be 0.05% of the river's temperature amplitude. The data showed that at 1 m, the streambed temperature fluctuations were still 12% of the river temperature amplitude. This depth extends more than 3.5 times further than would be expected if the signal were driven by pure conduction. This propagation of the river's temperature signal to greater depths corresponds to the rapid pumping of water into the streambed on a daily basis, which drives advective heat transport.

[46] At Hornsby Bend, the maximum thermal penetration depth occurs at night when the river stage is at its highest and the river temperature is at its coolest (Figures 8 and 9). Still, groundwater temperatures are always cooler than river water temperatures. If the timing of the dam releases were such that maximum stage was synchronous with the maximum river temperature at Hornsby Bend, deeper parts of the streambed would experience warmer temperatures since the temperature signal itself would be warmer, corresponding to a deeper influence of the warmer surface water. Even with the asynchrony at our site, the stage fluctuations and corresponding pumping of river water in and out of the streambed extend the thermal impacts deeper into the bed in the highly permeable area of the transect. In the lower permeability areas of the transect (toward the midline of the river and near the bank), penetration of the warm temperature signal is limited by the silt and clay deposits.

[47] Nearer to the Tom Miller Dam, which releases in the early afternoon, there may be synchronicity between the highest river temperature and highest river stage (greatest vertical flux into the streambed). This implies that at the dam, warm temperatures may penetrate much further than observed at Hornsby Bend, warming a much deeper extent of the streambed. This dependence on the synchronicity of releases and the diel cycle of river temperatures for maximum penetration of the thermal signal implies that there may be significant spatial and temporal variability in the penetration depth and amplitude of warm river temperatures into the streambed along the channel of a regulated river. An understanding of the influence of regulation on streambed temperature is important as temperature can act as a control on the vitality of hyporheic ecological processes.

## 6. Conclusions

[48] At Hornsby Bend in the lower Colorado River of Texas, dam regulation forces the river to gain and lose water daily rather than gain continuously. As a consequence, hyporheic zone dynamics is a strong function of distance from the bank, and flow paths in the bed and the

bank are multidimensional. The variability in magnitude and direction of instantaneous flux (or head gradients) is greatest at the bank and diminishes toward the middle of the channel. This variation is hysteretic at each point with the degree of hysteresis diminishing with distance from the bank toward the river midline. An important implication for future studies is that hyporheic measurements near the center of regulated channels likely underestimate the impact of dam releases. Moreover, the persistent across-channel variation in head gradients indicates that near-stream and hyporheic flow paths are multidimensional even when the river is either dominantly gaining or losing.

[49] Larger fluctuations near the bank correspond to both a greater depth of the hyporheic zone and longer exchange times for water being pumped in and out of the streambed during daily stage fluctuations. The hydraulically defined depth of the hyporheic zone increases from 0.5 to 3.5 m near the bank. In contrast, other large, unregulated rivers should have hyporheic zones that scale with the size of bedforms, which are typically only a few decimeters in dimension. Temperatures near the banks are strongly impacted as well. When the river is recharging the riparian aquifer each day, the river's thermal wave penetrates deep into the streambed. At a meter below the SWI, the amplitude of the temperature fluctuations is still 12% of the daily river temperature fluctuations.

[50] The regulation also impacts the water table of the adjacent bank for several meters into the shore. At 3.5 m into the bank, the water table fluctuations are 47% of the river stage fluctuations. A fitted exponential model predicts that even at a distance of 10 m inland from the river, the daily water table fluctuations will be 10% of the amplitude of the river stage fluctuations.

[51] If this river system were unregulated and under its natural base flow-fed regime, it would have a minimal or even absent hyporheic zone. Instead, the hyporheic zone extends at least 1 m into the streambed and several meters laterally into the river bank. The impacts of river regulation are far reaching primarily because the stage fluctuations force the hyporheic zone response to take place rapidly over large spatial scales. Further detailed observation and simulation is needed to fully understand the effects of dam releases on downstream hydrology, ecology, and biogeochemistry as well as the natural processes of the riparian aquifers.

[52] **Acknowledgments.** This research was made possible by the NSF REU grant EAR-0852029 at the Environmental Science Institute at the University of TX at Austin with additional support from the Geology Foundation at UT. We thank Kevin Anderson of the Austin Water Utilities Hornsby Bend-Center for Environmental Research for access and logistical support. Further thanks go to Robert Newton, Roger Gary, Michael Markowski, Mark Hagemann, Corinne Wong, and the other REU participants for assistance at UT, Smith College, and in the field. Comments from Ty Ferre and two anonymous reviewers helped improve the manuscript.

## References

- Amtzen, E. V., D. R. Geist, and P. E. Dresel (2006), Effects of fluctuating river flow on groundwater/surface water mixing in the hyporheic zone of a regulated, large cobble bed river, *Riv. Res. Appl.*, 22, 937–946, doi:10.1002/rra.947.
- Bencala, K. E. (2005), Hyporheic exchange flows, in *Encyclopedia of Hydrology Science*, edited by M. P. Anderson, pp. 1733–1740, John Wiley, New York.
- Boano, F., R. Revelli, and L. Ridolfi (2008), Reduction of the hyporheic zone volume due to the stream-aquifer interaction, *Geophys. Res. Lett.*, 35, L09401, doi:10.1029/2008GL033554.
- Boulton, A. J., S. Findlay, P. Marmonier, E. H. Stanley, and H. M. Valett (1998), The functional significance of the hyporheic zone in streams and rivers, *Annu. Rev. Ecol. Syst.*, 29, 59–81.
- Boutt, D. F., and B. J. Fleming (2009), Implications of anthropogenic river stage fluctuations on mass transport in a valley fill aquifer, *Water Resour. Res.*, 45, W04427, doi:10.1029/2007WR006526.
- Brunke, M., and T. Gonser (1997), The ecological significance of exchange processes between rivers and groundwater, *Freshwater Biol.*, 37, 1–33.
- Calles, O., L. Nyberg, and L. Greenberg (2007), Temporal and spatial variation in quality of hyporheic water in one unregulated and two regulated boreal rivers, *Riv. Res. Appl.*, 23(8), 829–842, doi:10.1002/rra.1015.
- Cardenas, M. B. (2008), Surface water-groundwater interface geomorphology leads to scaling of residence times, *Geophys. Res. Lett.*, 35(8), L08402, doi:10.1029/2008GL033753.
- Cardenas, M. B. (2009), Stream-aquifer interactions and hyporheic exchange in gaining and losing sinuous streams, *Water Resour. Res.*, 45, W06429, doi:10.1029/2008WR007651.
- Cardenas, M. B. (2010), Thermal skin effect of pipes in streambeds and its implications on groundwater flux estimation using diurnal temperature signals, *Water Resour. Res.*, 46, W03536, doi:10.1029/2009WR008528.
- Cardenas, M. B., and J. L. Wilson (2007a), Exchange across a sediment-water interface with ambient groundwater discharge, *J. Hydrol.*, 346, 69–80, doi:10.1016/j.jhydrol.2007.08.019.
- Cardenas, M. B., and J. L. Wilson (2007b), Dunes, turbulent eddies, and interfacial exchange with permeable sediments, *Water Resour. Res.*, 43(8), W08412, doi:10.1029/2006WR005787.
- Cardenas, M. B., and J. L. Wilson (2007c), Thermal regime of dune-covered sediments under gaining and losing water bodies, *J. Geophys. Res.*, 112, G04013, doi:10.1029/2007JG000485.
- Cardenas, M. B., and J. L. Wilson (2007d), Effects of current-bed form induced fluid flow on the thermal regime of sediments, *Water Resour. Res.*, 43(8), W08431, doi:10.1029/2006WR005343.
- Cardenas, M. B., and V. A. Zlotnik (2003), A simple constant-head injection test for streambed hydraulic conductivity estimation, *Ground Water*, 41(6), 867–871.
- Constantz, J. (1998), Interaction between stream temperature, streamflow, and groundwater exchanges in Alpine streams, *Water Resour. Res.*, 34(7), 1609–1615, doi:10.1029/98WR00998.
- Constantz, J. (2008), Heat as a tracer to determine streambed water exchanges, *Water Resour. Res.*, 44, W00D10, doi:10.1029/2008WR006996.
- Curry, R. A., J. Gehrels, D. L. G. Noakes, and R. Swainson (1994), Effects of river flow fluctuations on groundwater discharge through brook trout, *Salvelinus fontinalis*, spawning and incubation habitats, *Hydrobiologia*, 277(2), 121–134.
- Desilets, S. L. E., T. P. A. Ferre, and P. A. Troch (2008), Effects of stream-aquifer disconnection on local flow patterns, *Water Resour. Res.*, 44(9), W09501, doi:10.1029/2007WR006782.
- Findlay, S. (1995), Importance of surface-subsurface exchange in stream ecosystems- The hyporheic zone, *Limnol. Oceanogr.*, 40(1), 159–164.
- Francis, B. A., L. K. Francis, and M. B. Cardenas (2010), Water table dynamics and groundwater-surface water interaction during filling and draining of a large fluvial island due to dam-induced river stage fluctuations, *Water Resour. Res.*, 46, W07513, doi:10.1029/2009WR008694.
- Hancock, P. J. (2002), Human impacts on the stream-groundwater exchange zone, *Environ. Manage.*, 29(6), 763–781.
- Hanrahan, T. P. (2008), Effects of river discharge on hyporheic exchange flows in salmon spawning areas of a large gravel-bed river, *Hydrol. Proc.*, 22, 127–141, doi:10.1002/hyp.6605.
- Hatch, C. E., A. T. Fisher, J. S. Revenaugh, J. Constantz, and C. Ruehl (2006), Quantifying surface water-groundwater interactions using time series analysis of streambed thermal records: Method development, *Water Resour. Res.*, 42(10), W10410, doi:10.1029/2005WR004787.
- Hester, E. T., M. W. Doyle, and G. C. Poole (2009), The influence of in-stream structures on summer water temperatures via induced hyporheic exchange, *Limnol. Oceanogr.*, 54(1), 355–367.
- Lewandowski, J., G. Lischeid, and G. Nützmann (2009), Drivers of water level fluctuations and hydrological exchange between groundwater and surface water at the lowland River Spree (Germany): Field study and statistical analyses, *Hydrol. Proc.*, 23, 1–12, doi:10.1002/hyp.7277.

- Li, H. L., and J. J. Jiao (2003), Influence of the tide on the mean water table in an unconfined, anisotropic, inhomogeneous coastal aquifer, *Adv. Water Resour.*, 26(1), 9–16.
- Loheide, S. P., and J. D. Lundquist (2009), Snowmelt-induced diel fluxes through the hyporheic zone, *Water Resour. Res.*, 45, W07404, doi:10.1029/2008WR007329.
- Malcolm, I. A., C. Soulsby, A. F. Youngson, D. M. Hannah, I. S. McLaren, and A. Thorne (2004), Hydrological influences on hyporheic water quality: Implications for salmon egg survival, *Hydrol. Proc.*, 18(9), 1543–1560.
- McCallum, J. L., P. G. Cook, P. Brunner, and D. Berhane (2010), Solute dynamics during bank storage flows and implications for chemical base flow separation, *Water Resour. Res.*, 46, W07541, doi:10.1029/2009WR008539.
- Nielsen, P. (1990), Tidal dynamics of the water-table in beaches, *Water Resour. Res.*, 26(9), 2127–2134, doi:10.1029/90WR00726.
- Nilsson, C., and K. Berggren (2000), Alterations of riparian ecosystems caused by river regulation, *Bioscience*, 50(9), 783–792.
- Nilsson, C., C. A. Reidy, M. Dynesius, and C. Revenga (2005), Fragmentation and flow regulation of the world's largest river systems, *Science*, 308(5720), 405–408.
- Rotzoll, K., A. I. El-Kadi, and S. B. Gingerich (2008), Analysis of an unconfined aquifer subject to asynchronous dual-tide propagation, *Ground Water*, 46(2), 239–250, doi:10.1111/j.1745-6584.2007.00412.x.
- Sawyer, A. H., M. B. Cardenas, A. Bomar, and M. Mackey (2009), Impact of dam operations on hyporheic exchange in the riparian zone of a regulated river, *Hydrol. Proc.*, 23, 2129–2137, doi:10.1002/hyp.7324.
- Shepherd, B. G., G. F. Hartman, and W. J. Wilson (1986), Relationships between stream and intragravel temperatures in coastal drainages, and some implications for fisheries workers, *Can. J. Fish. Aquat. Sci.*, 43(9), 1818–1822.
- Singh, S. K. (2004), Aquifer response to sinusoidal or arbitrary stage of semi-pervious stream, *J. Hydraul. Eng.*, 130(11), 1108–1118, doi:10.1061/(ASCE)0733-9429(2004)130:11(1108).
- Swanson, T. E., and M. B. Cardenas (2010), Diel heat transport within the hyporheic zone of a pool-riffle-pool sequence of a losing stream and evaluation of models for fluid flux estimation using heat, *Limnol. Oceanogr.*, 5(4), 1741–1754, doi:10.4319/lo.2010.55.4.1741.
- Vervier, P., J. Gibert, P. Marmonier, and M. J. Doleolivier (1992), A perspective on the permeability of the surface fresh water-groundwater ecotone, *J. North Am. Benthol. Soc.*, 11(1), 93–102.
- Ward, J. V., and J. A. Stanford (1982), Thermal responses in the evolutionary ecology of aquatic insects, *Annu. Rev. Entomol.*, 27, 97–117.
- White, D. S. (1993), Perspectives in defining and delineating hyporheic zones, *J. North Am. Benthol. Soc.*, 12(1), 61–69.
- Winter, T. C., J. W. Harvey, O. L. Franke, and W. A. Alley (1998), Groundwater and surface water: A single resource, *U.S. Geol. Surv. Circ.*, 1139, 1–79.
- Wondzell, S. M., and F. J. Swanson (1996), Seasonal and storm dynamics of the hyporheic zone of a 4th-order mountain stream. I: Hydrologic processes, *J. North Am. Benthol. Soc.*, 15, 3–19.
- Wondzell, S. M., M. N. Gooseff, and B. L. McGlynn (2010), An analysis of alternative conceptual models relating hyporheic exchange flow to diel fluctuations in discharge during baseflow recession, *Hydrol. Proc.*, 24(6), 686–694, doi:10.1002/hyp.7507.

M. B. Cardenas, J. D. Nowinski, A. H. Sawyer, and T. E. Swanson, Geological Sciences, University of Texas at Austin, 1 University Station C9000, Austin, TX 78712, USA.

K. E. Gerecht, and A. J. Guswa, Picker Engineering Program, Smith College, Northampton, MA 01063, USA.